Carbon Nanotube Electron Windmills: A Novel Design for Nanomotors

S. W. D. Bailey, I. Amanatidis, and C. J. Lambert
Department of Physics, Lancaster University, Lancaster LA1 4YB, United Kingdom
(Received 20 March 2008; published 24 June 2008)

We propose a new drive mechanism for carbon nanotube (CNT) motors, based upon the torque generated by a flux of electrons passing through a chiral nanotube. The structure of interest comprises a double-walled CNT formed from, for example, an achiral outer tube encompassing a chiral inner tube. Through a detailed analysis of electrons passing through such a ''windmill,'' we find that the current, due to a potential difference applied to the outer CNT, generates sufficient torque to overcome the static and dynamic frictional forces that exist between the inner and outer walls, thereby causing the inner tube to rotate.

DOI: 10.1103/PhysRevLett.100.256802 PACS numbers: 85.65.+h, 61.46.Fg, 68.35.Af, 73.63.Fg

The evolution from microelectronics to nanoelectronics, as exemplified by the exponential growth in mobile communications and personal computing, is paralleled by the more recent miniaturization of mechanical devices, which are currently undergoing a transition from commercially available microelectromechanical structures (MEMSs) to nanometer-scale nanoelectromechanical structures (NEMSs). Whereas microfabricated motors, actuators and oscillators [1] are typically manufactured by conventional semiconductor processing techniques, their nanoscale counterparts are more difficult to realize.

An early example of an artificial NEMS [2,3] is based on a telescoping structure formed from multiwalled carbon nanotubes (MWCNTs). These structures possess novel electrical properties [4] and extremely low intershell friction [5]. The latter discovery led to the idea of carbon nanotube (CNT) nanomechanical oscillators [5–9] with gigahertz operation frequencies, which is beyond the reach of MEMS oscillators [10]. The ultralow intershell friction in MWCNTs also underpins recently developed CNT-based nanomotors [11,12], which involve a MWCNT whose outer shell is clamped to two metallic anchor pads and whose inner shell (or shells) is free to rotate or oscillate. A metallic plate is deposited on the mobile shell and movement is induced via an electrostatic interaction between the metallic plate and external gates.

The aim of the present Letter is to propose a new dc drive mechanism for CNT-based motors [13]. For all such nanomechanical devices analyzed to date, the static forces can roughly be classified as elastic, electrostatic, friction and van der Waals. In this Letter, we propose a new force which has so far been ignored in the NEMS literature. This force provides a new ''electron-turbine'' drive mechanism for CNT-based nanomotors and obviates the need for metallic plates and gates in the nanomotor of [11,12]. To understand the origin of this force, consider the structure shown in Fig. 1(a), which comprises a double-walled CNT, formed from an achiral $(18, 0)$ outer tube clamped to external electrodes and a chiral $(6, 4)$ inner tube. As in [11,12], the central region of the outer tube has been removed to expose the free-to-rotate, chiral inner tube. The proposed force arises when a dc voltage is applied between the external electrodes, which produces a ''wind'' of electrons, for example, from left to right. The incident electron flux (from the achiral CNT) possesses zero angular momentum, whereas after interacting with the chiral nanotube, the outgoing current carries a finite angular momentum. By Newton's third law, this flux of angular momentum produces a tangential force (and an associated torque) on the inner nanotube, causing it to rotate.

Figure 1(b) shows an even simpler version of this motor, which we refer to as a CNT ''drill,'' which comprises an achiral outer tube clamped to an external electrode and a free-to-rotate, chiral inner tube contacted to a mercury bath as in [14].

The main question is whether this new force is sufficient to overcome frictional forces between the inner and outer tube. The central result of our calculations is that, for moderate voltages, the tangential force produced by the electron wind can significantly exceed the frictional forces; therefore, electron windmills provide a viable alternative to electrostatic nanomotors realized to date. This result is illustrated in Fig. 2(a), which shows the tangential force (F_{motor}) as a function of the applied voltage (ϕ) exerted on the $(18, 0)@(6, 4)$ drill of Fig. 1(b), where @ indicates

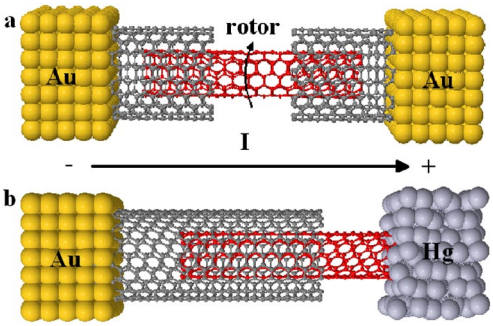

FIG. 1 (color online). The proposed nanomotor (a) and nanodrill (b) formed from an inner $(6, 4)$ CNT (red) and an outer $(18, 0)$ CNT (light gray). The nanomotor is attached to gold electrodes, which act as reservoirs of electrons, whereas the nanodrill has one end contacted to a mercury electrode.

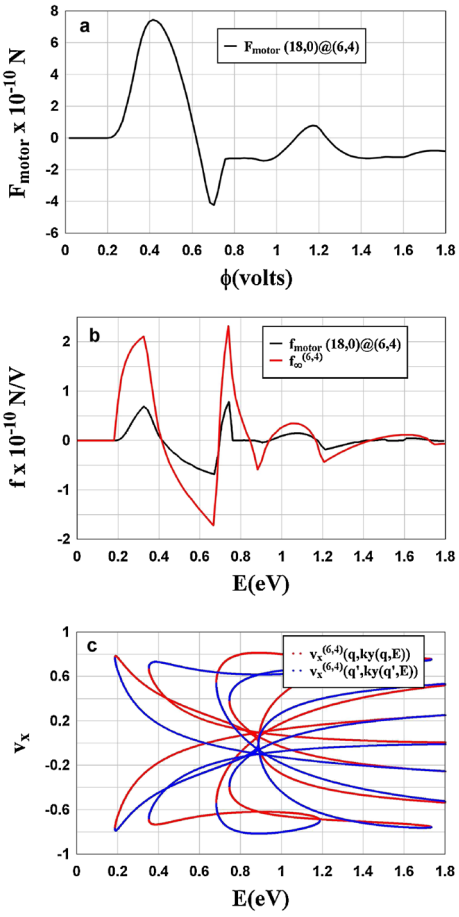

FIG. 2 (color online). (a) The tangential force (F_{motor}) exerted on a $(18, 0)@(6, 4)$ nanodrill as a function of the voltage ϕ. (b) The black curve shows the computed tangential force per volt $f_{\text{motor}}(E)$ for the $(18, 0)@(6, 4)$ drill, whose integral yields the curve in Fig. 1(a), in accordance with Eq. (7). For comparison, the red or light gray curve shows the quantity $f_{\infty}^{(6,4)}(E)$ of Eq. (12), which is proportional to the total tangential velocity carried by all right-moving channels of energy E in an infinite $(6, 4)$ chiral CNT. (c) A "fan diagram" showing the tangential velocities $v_x^{(6,4)}(q, k_y(q, E))/v_F$ carried by right-moving channels q (red or light gray) and left-moving channels q' (blue or dark gray) of an infinite $(6, 4)$ chiral CNT. The red or light gray curves sum to yield the red or light gray curve of (b), in accordance with Eq. (10).

"inside." In this example, the number of overlap atoms (N_{atoms}) between the inner $(6, 4)$ and the outer $(18, 0)$ CNT is approximately 4000 and since the static friction is $F_{\text{exp}} \approx 10^{-15}$ N/atom [15], the total static friction is $F_c \approx 4 \times 10^{-12}$. Figure 2(a) shows that when ϕ is approximately 0.4 volts, F_{motor} exceeds F_c by almost 3 orders of magnitude.

To obtain the result of Fig. 2(a), we note that the momentum of an electron wave packet incident along a semi-infinite CNT is equal to the mass of the electron multiplied by its group velocity. To quantify the tangential momentum, consider an (n, m) CNT defined by a chiral vector $\mathbf{C_h} = n\mathbf{a_1} + m\mathbf{a_2}$ and a translation vector $\mathbf{T_r} = t_1\mathbf{a_1} + t_2\mathbf{a_2}$, where $(0 \le m \le n)$, $\mathbf{a_1}$, $\mathbf{a_2}$ are the lattice vectors, $t_1 = (2m + n)/d_r$ and $t_2 = -(2n + m)/d_r$ with d_r the greatest common divisor of $(2n + m, 2m + n)$.

For electrons with group velocity $\mathbf{v}$, we define the longitudinal component of the velocity to be $v_y = \mathbf{v} \cdot \mathbf{T_r}$ and the transverse to be $v_x = \mathbf{v} \cdot \mathbf{C_h}$. The quantized component k_x of the wave vector $\mathbf{k} = (k_x, k_y)$ parallel to the chiral vector satisfies

$$k_x^q = \frac{2\pi q}{L} \qquad (q = 1, \ldots, N_{\text{hex}}),$$

where $N_{\text{hex}} = 2L^2/(a^2 d_r)$ is the number of hexagons in the CNT unit cell with L the length of the chiral vector and a the length of the lattice vector. For a given value of the quantized wave vector k_x^q, the energy of an electron is a function $E(k_x^q, k_y)$ of the continuous longitudinal component k_y of the wave vector, which satisfies

$$-\frac{\pi}{|\mathbf{T_r}|} < k_y a < +\frac{\pi}{|\mathbf{T_r}|}.$$

For example, within a minimal tight-binding model of π bonding in graphene, with a parameterized tight-binding transfer integral γ, the 1D dispersion curves for such a CNT are given by

$$E(k_x, k_y) = \pm\gamma\Big(1 + 4\cos\frac{\sqrt{3}}{2}(k_x a\cos\theta - k_y a\sin\theta) \times \cos\frac{1}{2}(k_x a\sin\theta + k_y a\cos\theta) + 4\cos^2\frac{1}{2}(k_x a\sin\theta + k_y a\cos\theta)\Big)^{1/2}, \qquad (1)$$

where $\tan\theta = (n - m)/\sqrt{3}(n + m)$ (i.e., θ is $\pi/6$ minus the chiral angle). For all electrons of energy E moving along a 1D channel of quantum number q, the equation $E(k_x^q, k_y) = E$ can be solved to yield two E-dependent values of k_y, which we denote by $k_y(q, E)$ and $-k_y(q', E)$, corresponding to positive (i.e., right-moving) and negative (i.e., left-moving) longitudinal group velocities $v_y(q, k_y)$ and $v_y(q', -k_y)$ respectively, where $v_y(q, k_y) = (1/\hbar)\partial E(k_x^q, k_y)/\partial k_y$. The corresponding tangential group velocities are $v_x(q, k_y)$ and $v_x(q', -k_y)$ respectively, where $v_x(q, k_y) = (1/\hbar)\partial E(k_x^q, k_y)/\partial k_x^q$.

For an $(n', m')@(n, m)$ structure of the kind shown in Fig. 1, which is derived from a chiral (n, m) CNT inside an achiral (n', m') CNT, a right-moving electron of energy E incident along channel q, with tangential group velocity $v_x(q, k_y(q, E))$ will either be reflected into left-moving channels q' of the left CNT with tangential group velocities $v_x(q', -k_y(q', E))$ and reflection probability $R_{q'q}(E)$ or it will be transmitted into right-moving channels q' of the right CNT with tangential group velocities $v_x(q', k_y(q', E))$ and transmission probability $T_{q'q}(E)$.

The flux of tangential momentum into the motor is

$$P_{\text{motor}} = \frac{2m_e}{h}\int_{-\infty}^{\infty} dE[v_{\text{in}}(E) - v_{\text{out}}(E)][f_{\text{left}}(E) - f_{\text{right}}(E)], \tag{2}$$

where $f_{\text{left}}(E)$ and $f_{\text{right}}(E)$ are Fermi distributions for incoming channels from the left and right reservoirs and

$$v_{\text{in}} = \sum_q v_x(q, k_y(q, E)). \tag{3}$$

Furthermore,

$$v_{\text{out}}(E) = v_R(E) + v_T(E), \tag{4}$$

where

$$v_R(E) = \sum_{q'q}[v_x(q', -k_y(q', E))R_{q'q}(E)], \tag{5}$$

$$v_T(E) = \sum_{q'q}[v_x(q', k_y(q', E))T_{q'q}(E)]. \tag{6}$$

In these equations, q sums over incoming channels and q' sums over outgoing channels. Equation (2) is valid even if both CNTs are chiral. By symmetry, for the case considered here, where the outer CNT is achiral, $v_{\text{in}}(E) = 0$. It can also be demonstrated that for the case of total reflection, where $T_{q'q}(E) = 0$ (for all q', q), Eq. (4) yields $v_{\text{out}}(E) = 0$.

By Newton's third law, the net tangential force exerted on the inner chiral CNT is $F_{\text{motor}} = -P_{\text{motor}}$ and therefore

$$F_{\text{motor}} = \int_{-\infty}^{\infty} \frac{dE}{e} f_{\text{motor}}(E)[f_{\text{left}}(E) - f_{\text{right}}(E)], \tag{7}$$

where $f_{\text{motor}}(E)$ is the tangential force per volt due to electrons of energy E, given by

$$f_{\text{motor}}(E) = f_0[v_{\text{out}}(E) - v_{\text{in}}(E)]/v_F, \tag{8}$$

with f_0 the characteristic tangential force per volt, given by

$$f_0 = \frac{2m_e e}{h} v_F. \tag{9}$$

For metallic CNTs, $v_F = 9.35 \times 10^5$ m/s and therefore $f_0 = 4.12 \times 10^{-10}$ N/V. (The corresponding force at 1 V is $F_0 = 4.12 \times 10^{-10}$ N and is the natural unit of force introduced above.) We note that if $e\phi$ is the chemical potential difference between the reservoirs and if $e\phi$ is small compared with $k_B T$, then $[f_{\text{left}}(E) - f_{\text{right}}(E)] \approx e\phi[-\partial f(E)/\partial E]$, which reduces to $e\phi\delta(E - E_F)$ in the limit $k_B T \to 0$. On the other hand, if $k_B T$ is small compared with $e\phi$, then $[f_{\text{left}}(E) - f_{\text{right}}(E)]$ is of order unity within an energy interval of order $e\phi$ and zero outside this interval. In what follows, for the purpose of proving the viability of the proposed motor, we shall focus on the latter regime.

For an $(n', m')@(n, m)$ motor with an achiral (n', m') outer CNT, an upper bound for the tangential force is obtained by setting $v_{\text{in}} = 0$ and replacing v_{out} by the maximum possible tangential velocity carried by right-moving channels of an infinite (n, m) chiral CNT. In units of v_F this is given by

$$v_\infty^{(n,m)}(E) = \sum_q v_x^{(n,m)}(q, k_y(q, E))/v_F, \tag{10}$$

where $v_x^{(n,m)}(q, k_y(q, E))/v_F$ is the dimensionless tangential group velocity of a right-moving channel q of an infinite (n, m) CNT.

The flux of tangential momentum carried by these electrons yields an upper bound on the tangential force of the corresponding motor, given by

$$F_\infty^{(n,m)}(e\phi) = \int_{-e\phi/2}^{e\phi/2} \frac{dE}{e} f_\infty^{(n,m)}(E), \tag{11}$$

where $f_\infty^{(n,m)}(E)$ is the flux of tangential momentum per volt due to electrons of energy E, given by

$$f_\infty^{(n,m)}(E) = f_0 v_\infty^{(n,m)}(E). \tag{12}$$

The latter quantity is shown as the red curve in Fig. 2(b), whereas the black curve shows the tangential force per volt obtained by computing all scattering coefficients and evaluating Eq. (8).

To understand the origin of the oscillations in $f_\infty^{(n,m)}(E)$, the red curves in Fig. 2(c) show the values of $v_x^{(6,4)}(q, k_y(q, E))/v_F$ for right-moving channels. (For comparison, the blue curves show $v_x^{(6,4)}(q', k_y(q', E))/v_F$ for left-moving channels.) In Eq. (10), the label q sums over $N(E)$ open channels of the CNT, where $N(E)$ is an integer given by $N(E) = \sum_q$. Clearly $N(E)$ is a discontinuous function of E, which changes by an integer whenever new channels open or close. As shown by the red curves in Fig. 2(c), right-moving channels open or close in pairs and just as a pair of channels open, their tangential velocities cancel. Consequently, $v_\infty^{(6,4)}(E)$ is a continuous function of E, with a discontinuous first derivative.

The red (light gray) curve of Fig. 2(b) shows that the tangential velocity of right-moving electrons in an infinite chiral CNT is an oscillatory function of E, whose slope changes whenever new channels open. The black curve of Fig. 2(b) shows that these oscillations are also present in $f_{\text{motor}}(E)$. To compute $f_{\text{motor}}(E)$, we used a parameterized single-state π orbital Hamiltonian, based on a global fit to density functional results for graphite, diamond and C_2 as a function of the lattice parameter [16]. This gives good agreement with the single π orbital interaction between two carbon atoms separated by $d = 3.40$ Å predicted by [17] of 0.35 eV and is appropriate to our system, where the interwall separation is $d = 3.65$ Å. A recursive Greens function formalism was then used to evaluate the transmission matrix $\mathbf{t}$, describing the scattering of electrons of energy E from one end of the semi-infinite nanotube to the other [18].

The tangential force shown in Fig. 2(a) is obtained by integrating the black curve of Fig. 2(b) over the applied

voltage, in accordance with Eq. (7). The result depends slightly on the orientation of the inner tube relative to the outer tube; therefore, the results shown in Fig. 2(a) is averaged over all orientations. We have carried out calculations which demonstrate the viabilities of CNT motors and drills with a wide variety of chiralities and intertube couplings. The result is rather robust and does not depend strongly on the number of overlap atoms, provided the electrons evolving from the outer to the inner tube do not strongly back scatter. If the intertube coupling causes strong back scattering, then the tangential force is reduced, but oscillations of the form shown in Fig. 2(b) persist. Figure 2(b) demonstrates that the tangential force vanishes for energies below approximately 0.19 eV, since there are no open channels in the chiral (6, 4) CNT. It is interesting to note that a voltage threshold also occurs when the achiral outer CNT is chosen to be an armchair tube, because the two channels closest to the Fermi energy possess vanishing tangential velocities and therefore electrons in these channels cannot exert a tangential force. In all cases, the voltage threshold can be removed by tuning the Fermi energy to coincide with open channels of the outer CNT carrying a finite tangential velocity.

As well as comparing the tangential force of Fig. 2 with the static friction, it is also of interest to ask if F_{motor} can overcome the dynamical friction between the two CNTs [19–21]. For a spinning CNT with carbon atoms of mass m_c moving with a tangential velocity v_c, the dynamical friction force per carbon atom is [21] $m_c v_c/\tau$, where $\tau \approx 0.5$ ns. Equating the dynamical friction to F_{motor} yields a maximum tangential velocity of $v_{\mathrm{max}} \approx 10^7 \alpha/N_c$ ms^{-1}, where N_c is the number of overlap atoms and $\alpha = F_{\mathrm{motor}}/F_0$, where $F_0 = 4.1 \times 10^{-10}$ N is a natural unit of force (see below). This means that even for moderate voltages, the electron wind is sufficient to drive the inner tube to the mechanical breakdown velocity ($\approx 8 \times 10^3$ ms^{-1}) [21].

This demonstration, that an ''electron wind'' can cause a chiral ''CNT windmill'' to rotate, could lead to a range of applications [13]. By analogy with the occurrence of spin torques in magnetic point contacts and tunnel junctions [22,23], which have applications in nanoscale magnetic memory devices, one expects CNT windmills to have nanoscale memory applications. For example, a voltage pulse through a CNT motor would cause the inner element to rotate by a predetermined angle, which may be utilized in a switch or memory element. A rotating chiral CNT in contact with a reservoir of atoms or molecules could act as a nanofluidic pump. For the future, it will be of interest to examine other drive mechanisms for chiral CNT motors. For example, if the electrical contacts in Fig. 1 are replaced by reservoirs of atoms or molecules and a pressure difference is applied to drive the atoms or molecules from left to right, then the resulting transfer of angular momentum may also be sufficient to drive the motor, as could a flux of phonons resulting from a temperature difference between the ends of the device.

Finally, we note that other mechanisms for driving CNT motors have been proposed based on ac fields. In the case of [24] this involves the use of circularly polarized light, whereas [25] involves a Brownian ratchet. The force produced by the former is 2–3 orders of magnitude smaller than the drive mechanism discussed in the present Letter, while the latter requires a high-frequency drive voltage. We also note that Ref. [26] proposes similar rotation of helical molecules by passing electric current. In the latter paper the rotation is caused by the electron's acceleration in the helical nanowire.

This work is supported by the EPSRC, the EU, the DTI, and the North West Science Grid.

[1] W. Trimmer, *Micromechanics and MEMS: Classic and Seminal Papers to 1990* (IEEE Press, New York, 1997).
[2] J. Cummings and A. Zettl, Science **289**, 602 (2000).
[3] M.-F. Yu, B. I. Yakobson, and R. S. Ruoff, J. Phys. Chem. B **104**, 8764 (2000).
[4] I. M. Grace, S. W. Bailey, and C. J. Lambert, Phys. Rev. B **70**, 153405 (2004).
[5] A. N. Kolmogorov and V. H. Crespi, Phys. Rev. Lett. **85**, 4727 (2000).
[6] S. B. Legoas *et al.*, Phys. Rev. Lett. **88**, 076105 (2002).
[7] Q. Zheng and Q. Jiang, Phys. Rev. Lett. **88**, 045503 (2002).
[8] L. Forro, Science **289**, 560 (2000).
[9] P. A. Williams *et al.*, Phys. Rev. Lett. **89**, 255502 (2002).
[10] J. L. Rivera, C. McCabe, and P. T. Cummings, Nano Lett. **3**, 1001 (2003).
[11] A. M. Fennimore *et al.*, Nature (London) **424**, 408 (2003).
[12] B. Bourlon, D. C. Glattli, C. Miko, L. Forro, and A. Bachtold, Nano Lett. **4**, 709 (2004).
[13] C. J. Lambert, The Patents Office, Patents Directorate No. GB2422638 (2006).
[14] S. Franck, P. Poncharal, Z. L. Wang, and W. de Heer, Science **280**, 1744 (1998).
[15] A. Kis, K. Jensen, S. Aloni, W. Mickelson, and A. Zettl, Phys. Rev. Lett. **97**, 025501 (2006).
[16] D. Tománek and M. A. Schluter, Phys. Rev. Lett. **67**, 2331 (1991).
[17] R. Saito, G. Dresselhaus, and M. S. Dresselhaus, *Physical Properties of Carbon Nanotubes* (Imperial College Press, London, 1998).
[18] S. Sanvito, C. J. Lambert, and J. H. Jefferson, Phys. Rev. B **59**, 11 936 (1999).
[19] S. Zhang, W. K. Liu, and R. S. Ruoff, Nano Lett. **4**, 293 (2004).
[20] J. Servante and P. Gaspard, Phys. Rev. B **73**, 125428 (2006).
[21] J. Servante and P. Gaspard, Phys. Rev. Lett. **97**, 186106 (2006).
[22] S. I. Kiselev *et al.*, Nature (London) **425**, 380 (2003).
[23] G. D. Fuchs *et al.*, Phys. Rev. Lett. **96**, 186603 (2006).
[24] P. Kral and H. R. Sadeghpour, Phys. Rev. B **65**, 161401 (2002).
[25] Z. C. Tu and X. Hu, Phys. Rev. B **72**, 033404 (2005).
[26] P. Kral and T. Seideman, J. Chem. Phys. **123**, 184702 (2005).